Photoelectrochemical properties of cadmium chalcogenide sensitized textured porous zinc oxide plate electrodes

Supporting Information

Saim Emin,*,[†] **Mattia Fanetti,**[†] **Fatwa F. Abdi,**[‡] **Darja Lisjak,**[§] **Matjaz Valant,**[†] **Roel van de Krol,**[☼] **and Bernard Dam**[‡]

[†]Materials Research Laboratory, University of Nova Gorica, SI-5000, Slovenia
[‡]Materials for Energy Conversion and Storage (MECS), Department of Chemical Engineering, Delft University of Technology, 2600 GA Delft, The Netherlands
[§]Department for Materials Synthesis, Jožef Stefan Institute, 1000 Ljubljana, Slovenia
[☼]Helmholtz-Zentrum Berlin für Materialien und Energie Gmbh, Institute for Solar fuels, Hahn-Meitner-Platz 1, 14109 Berlin, Germany

*Correponding author. E-mail: saim.emin@ung.si, eminsaim@yahoo.com.

1. Calculation of theoretical photocurrent of ZnO/CdSe PEC.

Figure S1 shows the terrestrial reference solar spectrum (ASTM G-173-3),[1] where the spectral irradiance, $P_\lambda(\lambda)$ (mW cm^{-2} nm^{-1}), is plotted as a function of the wavelength, λ. From the spectral irradiance it can be calculated the photon flux at the Earth's surface via the following relation

$$P_T \int_0^\infty P_\lambda(\lambda)\mathrm{d}\lambda$$

(S1)

and integration of this equation in the range from 280 to 4000 nm yields 100 mW/cm^2 (AM 1.5 G). It is more convenient to use umber of photons instead of incident energy. The relation between incident photon flux, $I_\lambda(\lambda)$ (photons cm^{-2} nm^{-1} s^{-1}), and spectral irradiance is given by

$$I_\lambda(\lambda) = \frac{P_\lambda(\lambda)\lambda}{hc}$$

(S2)

where h is the Planck's constant and c is the speed of light in a vacuum. By knowing the IPCE and $I_\lambda(\lambda)$ values at the corresponding wavelength the photocurrent density, $J_\lambda(\lambda)$ (mA cm^{-2} nm^{-1}) can be calculated

$$J_\lambda = \mathrm{IPCE}(\lambda)I_\lambda(\lambda)e$$

(S3)

where e is the charge of an electron. Figure S1 shows the values of $J_\lambda(\lambda)$ vs. λ for CdSe-sensitized ZnO plate electrode. In order to relate $J_\lambda(\lambda)$ to our experimental data it is more convenient to calculate the photocurrent density to the threshold wavelength λ_{th} that can be calculated via the following integral

$$J_T = \int_0^{\lambda_{th}} J(\lambda)\mathrm{d}\lambda$$

(S4)

Figure 8 shows calculated J_T curve of CdSe-sensitized ZnO electrodes with a maximum value equal to 6.5 mA/cm^2. This value is much higher than the one obtained for ZnO and ZnO/CdS electrodes, which are 0.9 and 2.5 mA/cm^2, respectively. Comparing the experimental and
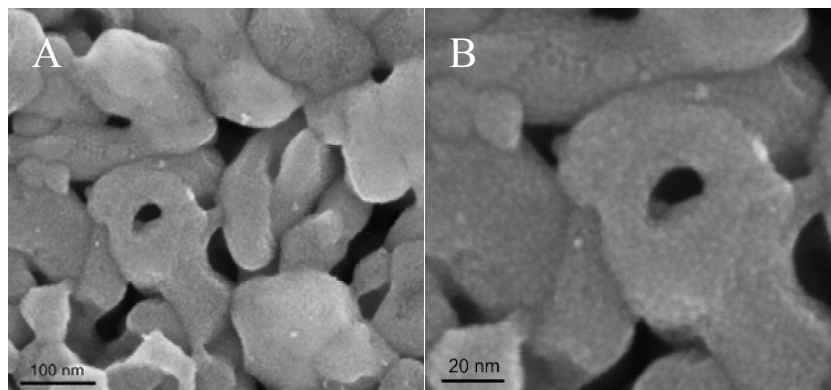
theoretically predicted values of the photocurrent density for ZnO/CdSe cell we can say that our cell reached 50% of the achievable photocurrent.

FigureS1. (a) Solar irradiance (P_λ) and solar photon flux (I_λ) at AM 1.5. (b) Solar photocurrent spectrum (J_λ) and integrated photocurrent (J_T) of CdSe-sensitized ZnO plate electrodes obtained using the IPCE values and the solar photon flux.

2. SEM images of ZnO plate electrodes

Figure S2. SEM images of ZnO plate electrodes prepared by using a substrate (FTO/glass) with (a) ~6×1.4 cm and (b) ~6×3.1 cm dimensions. Details regarding the electrochemical growth are given in the text.

ZnO working electrodes were prepared in a cell with a two-electrode configuration. F-doped SnO_2 coated glass substrates (Geomatec, Japan) with dimensions of ~6×1.4 cm (or ~6×3.1 cm) were used as both the anode and cathode. The deposition of $Zn_5(OH)_8Cl_2.H_2O$ plates was carried out at 75 ºC in an aqueous solution of 0.1M $ZnCl_2$ and 0.2 M H_2O_2. By applying a DC voltage of 2.6 V for 30 minutes we were able to deposit a ~6 μm thick $Zn_5(OH)_8Cl_2.H_2O$ film on the anode. The constant voltage and different electrode areas resulted in different current densities, which in turn affects the size of the ZnO plates (Fig. S2). Annealing of the $Zn_5(OH)_8Cl_2.H_2O$ electrode at 450 °C for 30 minutes gave porous ZnO plates.

3. SEM images of ZnO/CdS plate electrode

Figure S3 shows SEM images of CdS QDs sensitized ZnO plate electrodes.

Figure S3. SEM images of ZnO/CdS plates at different magnifications.

4. Diffuse reflectance spectra of ZnO plates illuminated in front and back configuration

Figure S4 shows the IPCE and diffuse reflectance spectra of ZnO plates illuminated in front and back configuration. The IPCE values for the cell illuminated from the front-side are lower than under back-side illumination. Upon front-side illumination of the ZnO film, most of the charge carriers were generated relatively far from the FTO substrate. This means they have to travel longer distances than under back-side illumination conditions. A lower front-side photocurrent therefore indicates that electron transport is limiting the overall photocurrent.[2-4] The difference in front- vs. back-side photocurrents cannot be attributed to lower light absorption under front-side illumination, for example due to light scattering effects. As shown in Fig. S4b, the diffuse reflectance under front-side illumination is lower than under back-side illumination, which means that the corresponding absorption is actually higher. Finally, we note that for these porous electrodes, no conclusions can be drawn on hole transport from front- vs. back-side illumination experiments; the distance that the holes have to travel to reach the electrolyte is the same in both cases.
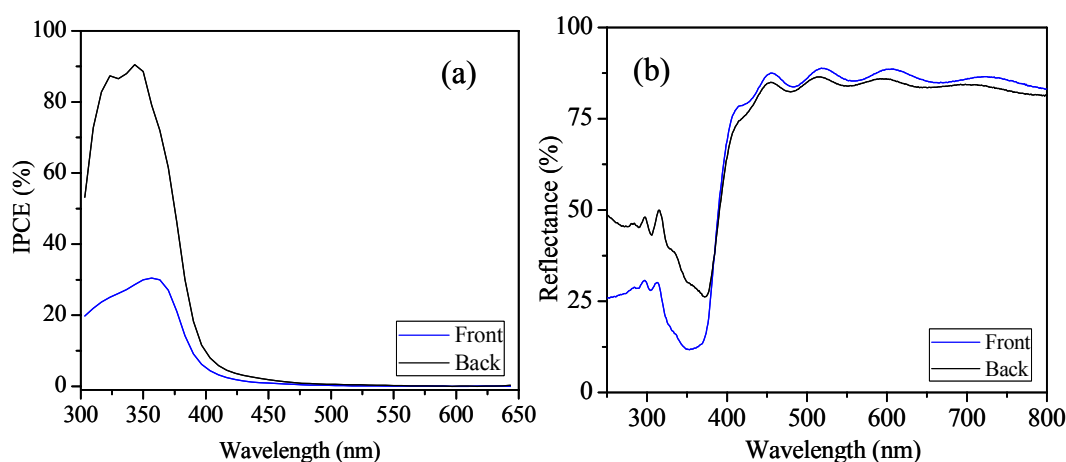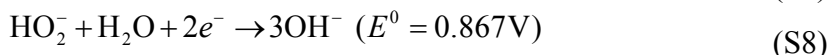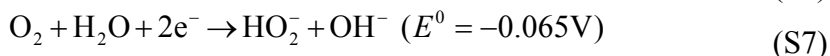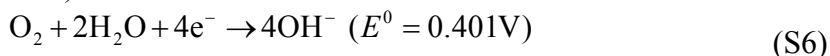

Figure S4. (a) IPCE and (b) diffuse reflectance spectra of ZnO plates illuminated in front and back configuration.

5. Possible alternative reactions in the presence of O$_2$

Since we did not purge the solution with inert gas, small amounts of dissolved oxygen gas may be present in the solution. This may lead to the homogeneous oxidation of a small fraction of the sulfite to sulfate:

$$2\mathrm{SO}_3^{2-} + \mathrm{O}_2 \rightarrow 2\mathrm{SO}_4^{2-} \tag{S5}$$

In alkaline aqueous solution the following sets of equations may proceed upon photoexcitation of the semiconductors (ZnO, CdS or CdSe):[5]

$$\mathrm{O}_2 + 2\mathrm{H}_2\mathrm{O} + 4\mathrm{e}^- \rightarrow 4\mathrm{OH}^- \ (E^0 = 0.401\mathrm{V}) \tag{S6}$$

$$\mathrm{O}_2 + \mathrm{H}_2\mathrm{O} + 2\mathrm{e}^- \rightarrow \mathrm{HO}_2^- + \mathrm{OH}^- \ (E^0 = -0.065\mathrm{V}) \tag{S7}$$

$$\mathrm{HO}_2^- + \mathrm{H}_2\mathrm{O} + 2e^- \rightarrow 3\mathrm{OH}^- \ (E^0 = 0.867\mathrm{V}) \tag{S8}$$

The potentials are given with respect to the normal hydrogen electrode (NHE). It is obvious that the formation of OH⁻ will maintain the alkalinity of the solutions, which eventually will facilitate the following reaction:

$$\mathrm{SO}_3^{2-} + 2\mathrm{OH}^- + 2\mathrm{h}^+(\mathrm{CB}) \rightarrow \mathrm{SO}_4^{2-} + \mathrm{H}_2\mathrm{O} \tag{S9}$$
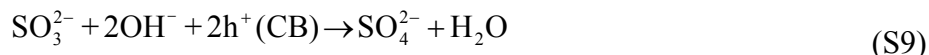
By removing any dissolved oxygen through purging, reactions (S5-S8) can be suppressed.

References

1   Evaluation, ASTM G-173-03 (available from: http://rredc.nrel.gov/solar/spectra/am1.5).
2   Liang, Y. Q.; Tsubota, T.; Mooiji, L. P. A.; Van de Krol, R. J. Phys. Chem. C 2011, 115, 17594-17598
3   Riha, S. C.; Frederick, S. J.; Sambur, J. B.; Liu, Y.; Prieto, A. L.; Parkinson, B. A.; ACS Appl. Mater. Interfaces 2011, 3, 58-66.
4   Abdi, F.F.; Krol, van de R. *J. Phys. Chem C* **2012**, *116*, 9398–9404.
5   Song, C.; Zhang, J. In *PEM Fuel Cell Electrocatalysts and Catalyst Layers*, Zhang, J., Eds.; Springer, London, **2008**, p 89–134.